
Masked Attention is All You Need for Graphs

David Buterez¹ Jon Paul Janet² Dino Oglic³ Pietro Lio¹

Abstract

Graph neural networks (GNNs) and variations of the message passing algorithm are the predominant means for learning on graphs, largely due to their flexibility, speed, and satisfactory performance. The design of powerful and general purpose GNNs, however, requires significant research efforts and often relies on handcrafted, carefully-chosen message passing operators. Motivated by this, we propose a remarkably simple alternative for learning on graphs that relies exclusively on attention. Graphs are represented as node or edge *sets* and their connectivity is enforced by masking the attention weight matrix, effectively creating custom attention patterns for each graph. Despite its simplicity, masked attention for graphs (MAG) has state-of-the-art performance on long-range tasks and outperforms strong message passing baselines and much more involved attention-based methods on over 55 node and graph-level tasks. We also show significantly better transfer learning capabilities compared to GNNs and comparable or better time and memory scaling. MAG has sub-linear memory scaling in the number of nodes or edges, enabling learning on dense graphs and future-proofing the approach.

1. Introduction

The field of geometric deep learning (GDL) seeks to describe, understand, and even “unify” deep learning strategies for data structures such as sets, grids, and graphs by leveraging the fundamental concepts of symmetry and invariance. A remarkably successful application of GDL is learning on graphs, abstractions that represent relationships between items of a set, and which naturally describe real-world phenomena such as social, biological, or transportation networks, as well as objects like molecules. In particular, deep

learning for molecules has the potential to accelerate and even revolutionise fields such as drug discovery and materials science, being one of the main factors behind the accelerated development of GDL, as well as one of the earliest (Duvenaud et al., 2015; Kearnes et al., 2016; Gilmer et al., 2017). General purpose learning on graphs is typically specified as an instance of *message passing*, an iterative algorithm where one must define a message function which aggregates information from a given node’s neighbourhood, as well as a node (possibly also edge) update function to incorporate the encoded messages.

Despite the overall success and wide adoption of GNNs, several fundamental problems have been highlighted over time. Firstly, although the message passing framework is highly customisable through user-defined, learnable message and node update functions, the design of novel layers is a difficult research problem, where improvements take years to achieve and often rely on hand-crafted operators. This is particularly the case for general purpose GNNs that do not exploit additional input modalities such as atomic coordinates. For example, principal neighbourhood aggregation (PNA) (Corso et al., 2020) is regarded as one of the most powerful message passing layers, but it is built using a collection of hand-picked neighbourhood aggregation functions, it requires a dataset degree histogram which must be pre-computed prior to learning, and further uses hand-picked degree scalars. Another example is given by Graph Attention Networks (GAT) (Veličković et al., 2018), one of the most popular graph layers and one of the earliest efforts to combine attention with GNNs. It has been shown, afterwards, that the original formulation of GAT has limited expressive power, and that a simple reordering of the operations can improve performance (Brody et al., 2022).

Secondly, the nature of message passing imposes certain limitations which have shaped most of the GNN literature. One of the most prominent examples is the readout function used to combine node-level representations into a single graph-level representation, and which is required to be permutation invariant with respect to the node order. Thus, the default choice for most GNNs remains a simple, non-learnable function such as sum, mean, or max, despite the potential limited expressivity. Recently, it has been shown that breaking this constraint can lead to improved performance, and might be acceptable in certain scenarios such as

¹Department of Computer Science and Technology, University of Cambridge, Cambridge, UK ²Molecular AI, BioPharmaceuticals R&D, AstraZeneca, Gothenburg, Sweden ³Centre for AI, BioPharmaceuticals R&D, AstraZeneca, Cambridge, UK.

learning on molecules, where the inputs can be presented in a canonical order (Buterez et al., 2022). Furthermore, expressive readout functions that are based on Set Transformers (Lee et al., 2019) have been shown to consistently improve performance of GNNs regardless of the underlying message passing algorithm (Buterez et al., 2022; 2023b).

Thirdly, the majority of GNN architectures are plagued by the well-known oversmoothing and oversquashing problems that limit the depth of GNNs, as well as difficulties in modelling long-range relationships, all of which are consequences of aggregating information from exponentially larger neighbourhoods (Alon & Yahav, 2021). The proposed solutions typically take the form of message regularisation schemes (Godwin et al., 2022; Zhao & Akoglu, 2020; Cai et al., 2021). However, there is generally not a consensus on the right architectural choices for deep GNNs. Separately, standard GNNs have also shown limitations in terms of transfer learning and strategies such as pre-training and fine-tuning, as opposed to other families of neural networks such as language models (Hu et al., 2020). For certain types of data and tasks, non-standard GNNs that leverage attention-based readouts are currently the only way to effectively perform transfer learning (Buterez et al., 2024; 2023a).

Perhaps due to the progress that message passing neural networks have enabled on a wide range of tasks, alternative paradigms for learning on graphs are relatively underdeveloped. The attention mechanism (Vaswani et al., 2017) is one of the main sources of innovation within graph learning, either by directly incorporating attention within message passing (Veličković et al., 2018; Brody et al., 2022), by formulating graph learning as a language processing task (Ying et al., 2021; Kim et al., 2022), or by combining standard GNN layers with an attention mechanism (Rampasek et al., 2022; Shirzad et al., 2023; Buterez et al., 2022; 2023b).

Here, we propose a novel graph learning framework characterised by its simplicity and lack of message passing layers, instead being based on a classical attention mechanism with masking to create custom attention patterns. Compared to some of the previous works that have formulated graph learning as a language modelling task, we take a different approach and consider graph learning as a learning task on *sets*, where the graph connectivity (i.e., adjacency matrix) is enforced by masking the pairwise attention weight matrix and allowing only values that correspond to graph connections. We term this architecture Masked Attention for Graphs (MAG) and demonstrate that it can be customised to propagate information across nodes (MAGN) or edges (MAGE). It is general purpose, in the sense that it only relies on the graph structure and possibly node and edge features, and it is not restricted to a particular domain such as chemistry. The simplicity of the architecture is further demonstrated by the fact that MAG does not use positional

or similar encodings, it does not encode graph structures as tokens or other language (sequence) specific concepts, and it does not require any pre-computations.

Despite its simplicity, MAG generally outperforms strong message passing baselines and much more involved attention-based algorithms. Our empirical evaluation covers long-range molecular benchmarks and over 55 tasks from different domains such as quantum mechanics, molecular docking, physical chemistry, biophysics, bioinformatics, computer vision, social networks, functional call graphs, and synthetic graphs. This emphasises the fact that the carefully-selected and hand-crafted nature of most message passing algorithms can be easily superseded by attention itself, without the need to explicitly define any operator. Beyond benchmarking, we also explore a recent research direction that showed the transformative benefits of transfer learning in drug discovery and quantum mechanics (Buterez et al., 2024). Here, we leverage a newly-published, refined version of the QM9 dataset at a higher level of theory (Fediai et al., 2023), and show that MAG is a viable and well performing transfer learning strategy, while GNNs are limited.

MAG is arguably one of the most straightforward ways to apply attention on graphs. Thanks to modern implementations of exact attention, MAG scales sub-linearly in terms of memory with the number of nodes (MAGN) or edges (MAGE), as it largely relies on (masked) self-attention. Although current libraries are not optimised for masked attention and many optimisations are possible (see Appendix A), both the training time and the memory consumption are competitive or even better than plain message passing.

2. Related Work

Graph neural networks with adaptive readouts – A recent research trend consists of following standard GNN layers with an attention-based pooling (readout) function, for example using the Set Transformer (Buterez et al., 2022; 2024; 2023b), or standard Transformers (Jain et al., 2021). The change to a more expressive readout function has provided consistent uplifts in most supervised learning tasks, and has enabled easy and effective transfer learning for molecules through a pre-training and fine-tuning workflow.

Transformers for graphs – One of the most popular approaches is the direct application of standard Transformers designed for language modelling to graphs. Graphormer (Ying et al., 2021) achieves this through an involved and computation-heavy suite of pre-processing steps, involving a centrality, spatial, and edge encoding. Graphormer models the mean readout function from GNNs through a special “virtual” node that is added to the graph and connected to every other node. Another approach within this paradigm is the Tokenized Graph Transformer (TokenGT) (Kim et al.,

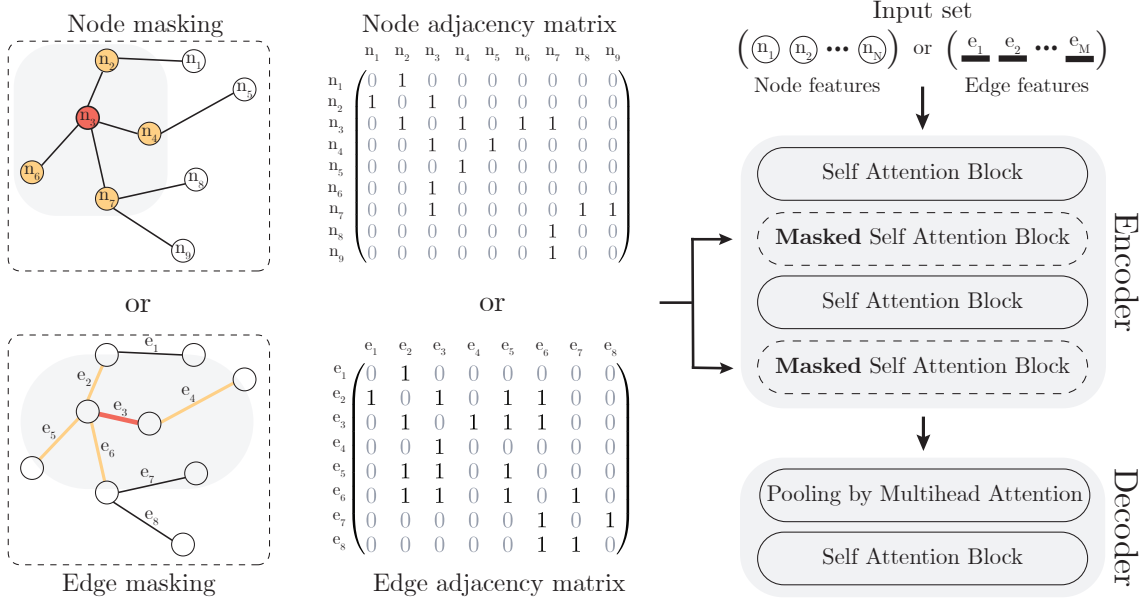


Figure 1. Overview of the Masked Attention for Graphs (MAG) architecture. An important aspect is the choice of processing the node feature set (MAGN) or the edge feature set (MAGE), and the appropriate masking algorithm. Conventional self attention blocks (S) can be alternated with masked variants (M) as desired (here, a choice of SMSM is depicted). The decoder is only required for graph-level tasks.

2022), which treats all the nodes and edges as independent tokens. To adapt sequence learning to the graph domain, TokenGT encodes the graph information using node identifiers derived from orthogonal random features or Laplacian eigenvectors, and learnable type identifiers for nodes and edges. Such models rely on embedding layers and are thus limited to integer node or edge features. Moreover, the high number of sequence-based architectures (e.g. Big Bird (Zaheer et al., 2020), Performer (Choromanski et al., 2021), etc.) represents a large unexplored territory for graphs. Spectral Attention Networks (Kreuzer et al., 2021) use a computationally-expensive positional encoding based on the Laplacian and two complementary attention mechanisms over nodes. A different philosophy is that of a message passing and Transformer hybrid. Such an approach is taken by the GraphGPS framework (Rampášek et al., 2022), which alternates message passing layers with Transformer layers. Like previous works, GraphGPS puts a large emphasis on different types of encodings, proposing and analysing positional and structural encodings, further divided into local, global, and relative encodings. Exphormer (Shirzad et al., 2023) is an evolution of GraphGPS which adds virtual global nodes and sparse attention based on expander graphs. While effective, such frameworks do still rely on message passing and are thus not purely attention-based solutions. Limitations include dependence on approximations (Performer for both, expander graphs for Exphormer), decreased performance when encodings (GraphGPS) or special nodes (Exphormer) are removed, and scalability (GraphGPS). Notably, Exphormer is the first work to consider custom attention patterns for graphs in the form of node-level neighbourhoods.

3. Preliminaries

Graphs – A graph is a tuple $\mathcal{G} = (\mathcal{V}, \mathcal{E})$ where \mathcal{V} represents the set of nodes, $\mathcal{E} \subseteq \mathcal{V} \times \mathcal{V}$ is the set of edges, and $N_n = |\mathcal{V}|$, $N_e = |\mathcal{E}|$. Nodes are associated with feature vectors \mathbf{x}_u of dimension d_n for all nodes $u \in \mathcal{V}$, and d_e -dimensional edge features \mathbf{e}_{uv} for all edges $e \in \mathcal{E}$. The node features are collected as rows in a matrix $\mathbf{X} \in \mathbb{R}^{N_n \times d_n}$, and similarly for edge features into $\mathbf{E} \in \mathbb{R}^{N_e \times d_e}$. The graph connectivity information can be represented as an adjacency matrix \mathbf{A} , where $\mathbf{A}_{uv} = 1$ if $(u, v) \in \mathcal{E}$ and $\mathbf{A}_{uv} = 0$ otherwise, although an edge list representation is often more practical. GNNs also define the neighbourhood of a node $u \in \mathcal{V}$ as $\mathcal{N}_u = \{v \mid (u, v) \in \mathcal{E} \vee (v, u) \in \mathcal{E}\}$. Many GNNs can be described as a form of message passing, which takes the general form of $m_u^{t+1} = \sum_{v \in \mathcal{N}_u} \text{message}_t(\mathbf{x}_u^t, \mathbf{x}_v^t, \mathbf{e}_{uv})$ and $x_u^{t+1} = \text{update}_t(x_u^t, m_u^{t+1})$ (Gilmer et al., 2017), where *message* and *update* are the message and node update functions, respectively, and t is the current time step. As described above, message passing is highly customisable, for example by novel definitions of the message and update functions, their inputs, or even adding new update steps such as the graph-level state embedding and update proposed in Chen et al. (2021) for multi-fidelity applications. For graph-level prediction tasks, a readout or pooling function \oplus must be used, aggregating all the learnt node representations: $\mathbf{x}_{\mathcal{G}} = \oplus_{u \in \mathcal{V}} (\mathbf{x}_u)$.

Set Transformer – The Set Transformer is an encoder-decoder attention-based architecture for learning on sets. It leverages the scaled dot product and multihead attention

Algorithm 1: Node masking algorithm, where the inputs follow PyTorch Geometric conventions.

```

1 from torch_geometric import unbatch_edge_index
2 function node_mask(b_ei, b_map, B, M)
3     # b_ei is the batched edge index
4     # b_map maps nodes to graphs
5     # B, M batch, respectively mask size
6     mask ← torch.full(size=(B, M, M), fill=False)
7     graph_idx ← b_map.index_select(0, b_ei[0, :])
8     eis ← unbatch_edge_index(b_ei, b_map)
9     ei ← torch.cat(eis, dim=1)
10    mask[graph_idx, ei[0, :], ei[1, :]] ← True
11    return ~mask

```

mechanisms proposed in Vaswani et al. (2017) to define multihead attention blocks (MABs), self attention blocks (SABs), and pooling by multihead attention (PMA) blocks. We do not recapitulate the definition of multihead attention and assume instead that a function Multihead ($\mathbf{Q}, \mathbf{K}, \mathbf{V}$) is available (for query, key, and value matrices, respectively). The original Set Transformer is given by $\text{ST}(\mathbf{X}) = \text{Decoder}(\text{Encoder}(\mathbf{X}))$ with:

$$\text{MAB}(\mathbf{X}, \mathbf{Y}) = \mathbf{H} + \text{Linear}_\phi(\mathbf{H}) \quad (1)$$

$$\text{and } \mathbf{H} = \mathbf{X} + \text{Multihead}(\mathbf{X}, \mathbf{Y}, \mathbf{Y}), \quad (2)$$

$$\text{SAB}(\mathbf{X}) = \text{MAB}(\mathbf{X}, \mathbf{X}), \quad (3)$$

$$\text{Encoder}(\mathbf{X}) = \text{SAB}^n(\mathbf{X}), \quad (4)$$

$$\text{PMA}_k(\mathbf{Z}) = \text{MAB}(\mathbf{S}_k, \text{Linear}_\phi(\mathbf{Z})), \quad (5)$$

$$\text{Decoder}(\mathbf{Z}) = \text{Linear}_\phi(\text{SAB}^n(\text{PMA}_k(\mathbf{Z}))). \quad (6)$$

and where Linear_ϕ is a linear layer followed by an activation function ϕ , $\text{SAB}^n(\cdot)$ represents n subsequent applications of a SAB, and \mathbf{S}_k is a tensor of k learnable seed vectors that are randomly initialised (PMA $_k$ outputs k vectors) (Buterez et al., 2023b). Notably, the original Set Transformer is designed exclusively for learning on sets, uses layer normalisation (LN) in a post-LN fashion (Xiong et al., 2020a), and does not use any form of positional or structural encodings.

Efficient attention – Recently, Flash attention has enabled exact attention with linear memory scaling and faster training and inference (up to x10) thanks to more efficiently utilising the architecture of modern graphics processing units (GPUs) (Dao et al., 2022; Dao, 2023). For self-attention, an exact attention implementation has also been developed that scales with the square root of the sequence length in terms of memory, and has comparable run time with standard implementations (Rabe & Staats, 2021).

4. Masked attention for graphs

We formulate graph learning as a learning problem on *sets*. The main learning mechanism consists of applying attention directly to the node or edge feature matrix by means of SABs. We propose *masking* the pairwise attention weight

matrix according to the node or edge adjacency information in order to incorporate the graph structure. We call this approach Masked Attention for Graphs (MAG).

Inputs – MAG supports two main ways of information propagation: (1) on nodes (MAGN), more specifically on the node feature matrix \mathbf{X} , or (2) on edges (MAGE), i.e. on the edge feature matrix \mathbf{E} .

Masking – We extend the Set Transformer with masked equivalents of the MAB and SAB (MSAB). Practically, this means supplying the new blocks with a mask tensor of shape $B \times N_d \times N_d$ for MAGN and $B \times N_e \times N_e$ for MAGE, where B is the batch size. In a naive implementation, masking simply means replacing the targeted values of the scaled QK^T product with negative infinity (or a very large negative value for stability) before softmax (Appendix F for the equation). The correct mask for each batch is different and must thus be computed on the fly. For MAGN, the mask allows only adjacent nodes. In other words, the $N_d \times N_d$ portion of the mask corresponds directly to the node adjacency matrix (Algorithm 1). For MAGE, the mask operates on the set of edges and must allow only edges that share a common node. While this computation is not as trivial as the MAGN mask, both kinds of masks can be efficiently computed using exclusively tensor operations (Algorithm 2).

Architecture – At a high level, a complete MAG model takes the form of an encoder where MSAB and SAB blocks are alternated as desired, with a PMA-based decoder (Figure 1). Compared to the Set Transformer, we have also adapted MAG to use a pre-LN architecture with layer or batch normalisation and optionally include multi-layer perceptrons (MLPs) after multihead attention. For graph-level tasks, the PMA module of the Set Transformer acts as an equivalent to the readout function in GNNs, but fully based on attention, while for node-level tasks PMA is not required.

5. Experiments

Our evaluation encompasses: (1) an extensive suite of over 55 benchmarks from various domains, where the goal is to compare MAG with representative message passing networks (GCN, GAT, GATv2, GIN, and PNA) and Transformers for graphs (Graphormer, TokenGT). Due to space limitations, we cannot present the results for all methods in the main part of the paper, so we select the most representative ones based on the task, with the rest presented in the Appendix. Graphormer and TokenGT are applicable only to a subset of tasks due to limitations discussed in Related Work. They also fail for many datasets due to very high memory requirements (CPU and/or GPU). We cover long-range tasks (Section 5.1), node-level tasks (Section 5.2) and graph-level tasks (Section 5.3). (2) A transfer learning performance evaluation (Section 5.4) based on a new, refined

Algorithm 2: Edge masking algorithm, where the inputs follow PyTorch Geometric conventions. \mathbf{T} is the transpose. Helper functions are explained in Appendix B.

```

1 from mag import consecutive, first_unique_index
2 function edge_adjacency(b_ei)
3     E ← b_ei.size(1)
4     source_nodes ← b_ei[0]
5     target_nodes ← b_ei[1]
6
7     # unsqueeze and expand
8     exp_src ← source_nodes.unsqueeze(1).exp((-1, E))
9     exp_trg ← target_nodes.unsqueeze(1).exp((-1, E))
10
11     src_adj ← exp_src == T(exp_src)
12     trg_adj ← exp_trg == T(exp_trg)
13     cross ← (exp_src == T(exp_trg)) logical_or
14             (exp_trg == T(exp_src))
15
16     return (src_adj logical_or trg_adj logical_or cross)
17 function edge_mask(b_ei, b_map, B, M)
18     mask ← torch.full(size=(B, M, M), fill=False)
19     edge_to_graph ← b_map.index_select(0, b_ei[0, :])
20
21     edge_adj ← edge_adjacency(b_ei)
22     ei_to_original ← consecutive(
23         first_unique_index(edge_to_graph), b_ei.size(1))
24
25     edges ← edge_adj.nonzero()
26     graph_idx ← edge_to_graph.idx_select(0, edges[:, 0])
27     coord_1 ← ei_to_original.idx_select(0, edges[:, 0])
28     coord_2 ← ei_to_original.idx_select(0, edges[:, 1])
29
30     mask[graph_idx, coord_1, coord_2] ← True
31     return ~mask

```

Table 1. Test set mean absolute error (MAE) or average precision (AP) for two long-range molecular benchmarks. All the results except for MAGE are extracted from (Tönshoff et al., 2023). The number of layers for PEPT-STRUCT, respectively PEPT-FUNC is given as (-/·).

Dataset	GCN (6/6)	GIN (10/8)	GraphGPS (8/6)	Exphormer (4/8)	MAGE (3/4)
PEPT-STRUCT (MAE ↓)	0.2460 ± 0.0007	0.2473 ± 0.0017	0.2509 ± 0.0014	0.2481 ± 0.0007	0.2453 ± 0.0003
PEPT-FUNC (AP ↑)	0.6860 ± 0.0050	0.6621 ± 0.0067	0.6534 ± 0.0091	0.6527 ± 0.0043	0.6863 ± 0.0044

Table 2. Test set Matthews correlation coefficient (MCC) for 3 node-level classification tasks, presented as mean ± standard deviation from 5 different runs. The highest mean values are highlighted in bold.

Dataset	GCN	GAT	GATv2	GIN	PNA	MAGN
PPI ↑	0.47 ± 0.02	0.82 ± 0.03	0.72 ± 0.39	0.35 ± 0.02	0.83 ± 0.01	0.99 ± 0.00
CITeseer ↑	0.30 ± 0.04	0.19 ± 0.03	0.21 ± 0.05	0.23 ± 0.03	0.01 ± 0.02	0.54 ± 0.02
CORA ↑	0.48 ± 0.06	0.37 ± 0.01	0.43 ± 0.04	0.39 ± 0.02	0.04 ± 0.05	0.70 ± 0.02

variant of QM9 and following the recent framework proposed by Buterez et al. (2024). (3) The time and memory characteristics for all discussed methods (Section 5.5).

5.1. Long-range tasks

Graph learning with Transformers has traditionally been evaluated on long-range graph benchmarks (LRGB) (Dwivedi et al., 2022). However, it was recently shown that simple GNNs outperform most attention-based methods (Tönshoff et al., 2023). Nonetheless, we evaluated MAGE on two long-range molecular tasks (Table 1) and conclude that it outperforms GraphGPS, Exphormer, GCN, and GIN. Despite using half the number of layers as other methods or less, MAGE matches the 2nd model on the PEPT-STRUCT leaderboard, and is within the top 5 for PEPT-FUNC (as of January 2024). Remarkably, MAG is the only top method that is exclusively based on attention (i.e. no message passing or hybrid), does not use any positional or similar encoding, and is general purpose (i.e. not specifically built for molecules). We also did not use hyperparameter optimisation or sophisticated schedulers (Appendix C).

5.2. Node-level tasks

Generally, node-level tasks take the form of citation networks of different sizes, and are not as varied as graph-level problems. Nonetheless, they represent an interesting case for MAG as PMA is not needed. Here, we selected 3 representative datasets: PPI, CITeseer, and CORA. In particular, MAGN is the most natural choice as it works over node representations. Our results indicate that MAGN is the best performing method by a large margin (Table 2). Graphormer and TokenGT are not available for node-level classification, and they would not work due to the large graph sizes.

5.3. Graph-level tasks

Graph-level tasks are generally more varied, as they often originate from different domains and require a readout function for GNNs and a PMA module for MAG. Here, we do not focus on the differences between readouts and instead choose a reasonably strong baseline (4-layer GNNs and mean readout; Appendix C for the experimental setup). A more granular evaluation of readouts has been done by (Buterez et al., 2022), concluding that the difference between readouts is small for most tasks.

QM9 is a quantum mechanics dataset consisting of 133,885 small organic molecules and 19 regression targets given by quantum properties (Ramakrishnan et al., 2014). We report results for all 19 targets in Table 3, with GCN and TokenGT separately in Appendix D due to limited space. We observe that for 15 out of 19 properties, MAGE is the best performing method. For the dipole moment (μ), PNA is better by a slight margin, while for HOMO, LUMO, and the HOMO-LUMO gap ($\Delta\epsilon$), Graphormer is stronger. We expect that attention-based methods would be the best suited for intensive and localised properties like the HOMO and LUMO, which agrees with recent literature on this topic (Buterez et al., 2023b). The fact that MAGE is not as competitive on these tasks could be explained by MAGE converging quicker than other methods and getting stuck in local minima, especially for HOMO/LUMO which take a long time to converge for most methods. We report the results of altering the number and order of attention blocks in Appendix I.

DOCKSTRING (García-Ortegón et al., 2022) is a recent drug discovery data collection consisting of molecular docking scores for 260,155 small molecules and 5 high-quality targets from different protein families that were selected as a regression benchmark, with different levels of difficulty: PARP1 (enzyme, easy), F2 (protease, easy to medium), KIT (kinase, medium), ESR2 (nuclear receptor, hard), and PGR (nuclear receptor, hard). The tasks are expected to be challenging, as the docking score depends on the 3D structure of the ligand–target complex. Furthermore, a cluster split into train (221,274 molecules) and test (38,881 molecules) sets is provided, ensuring a more difficult and meaningful benchmark. We have selected a random subset of 19,993 molecules from the original train set as a validation set (the test set is not modified). We report results for the 5 targets in Table 3 and observe that MAGE is the strongest method for 4 of the tasks. Remarkably, MAGE matches or outperforms the strongest methods in the original manuscript (Attentive FP, a GNN based on attention, Xiong et al., 2020b) despite using 20,000 less training molecules. Moreover, while the other methods are competitive for the 4 easy or medium difficulty tasks, MAGE outperforms the others by a large margin for the most difficult target (PGR).

We further extend our evaluation with a collection of datasets that covers multiple domains such as bioinformatics, physical chemistry, computer vision, social networks, functional call graphs, and synthetic graphs (Tables 3 to 5). We observe that MAGE and MAGN are competitive with the other methods and in most cases better.

5.4. Transfer learning

We follow the recipe recently outlined for drug discovery and quantum mechanics by Buterez et al. (2024). Here, we leverage a recently-published refined version of the QM9

HOMO and LUMO energies (Fediai et al., 2023), which provides alternative DFT calculations based on the correlation-consistent basis set aug-cc-DZVP and the PBE functional, as well as calculations at the (more accurate) eigen-value-self-consistent GW level of theory. The transfer learning setup consists of randomly selected training, validation, and test sets of 25K, 5K, and respectively 10K molecules with GW calculations (from the total 133,885). As outlined by Buterez et al. (2024), transfer learning can be performed in *transductive* or *inductive* setups. In the transductive case, test set DFT-level measurements are used for pre-training, while in the inductive setting they are not. Here, we perform transfer learning by pre-training a model on the DFT target for a fixed number of epochs and then fine-tuning it on the subset of 25K GW calculations. In the transductive case, pre-training occurs on the full set of 133K DFT calculations, while in the inductive case the DFT test set values are removed (note that the evaluation is done on the test set GW values). The results (Table 6) indicate that MAGE improves thanks to transfer learning from DFT by 45% (HOMO) and 53% (LUMO) in the challenging inductive case, with 10 to 20-fold improvements for the transductive case, while GNNs improve only by a modest amount.

5.5. Time and memory utilisation

In MAG, the most computation-intensive component is the encoder. All encoder blocks perform (masked) self attention, which can be efficiently implemented with $\mathcal{O}(\sqrt{N})$ memory complexity (N_n, N_e for MAGN, respectively MAGE). The time complexity is as for standard attention. The decoder PMA encodes cross-attention between the full set outputted by the encoder and a set of learnable k vectors, benefitting from Flash attention (linear memory and time scaling). A decoder with a single PMA block and $k = 1$, as used here, is even more efficient. The mask tensor requires $B \times N^2$ memory (Appendix A for a solution). However, it does not require gradients and MAGE runs with up to $N_e \approx 30,000$ edges on a consumer GPU with 24GB. Indeed, we report competitive time and memory utilisation (Table 7).

6. Discussion

We presented an end-to-end approach that leverages attention in a novel way for learning on graphs and demonstrated its effectiveness relative to message passing and more involved attention-based methods. Our approach is end-to-end in the sense that it replaces both message passing and readout/pooling functions with attention mechanisms. The former is facilitated by modularly stacking self and masked attention blocks (node or edge-based masking). In the future, node- and edge-masked blocks might be interspersed. Both node and edge masked attention mechanisms can be implemented using a few lines of code (Algorithms 1 and 2).

Table 3. Test set root mean squared error (RMSE, standard for quantum mechanics) QM9, and R^2 for the rest of tasks, presented as mean \pm standard deviation from 5 different runs. The lowest (QM9) and highest (rest) mean values are highlighted in bold. Only one of Graphormer/TokenGT was chosen for spacing reasons, based on competitiveness and lack of out-of-memory errors (OOM). Any results not displayed here (e.g. GCN, TokenGT) are available in Appendix D.

	Property	GAT	GATv2	GIN	PNA	Graphormer	MAGE
QM9	μ \downarrow	0.61 \pm 0.00	0.61 \pm 0.01	0.61 \pm 0.00	0.57 \pm 0.00	0.63 \pm 0.00	0.61 \pm 0.02
	α \downarrow	2.66 \pm 0.25	1.86 \pm 0.28	1.18 \pm 0.10	1.00 \pm 0.02	0.57 \pm 0.16	0.48 \pm 0.01
	ϵ_{HOMO} \downarrow	0.12 \pm 0.00	0.12 \pm 0.00	0.12 \pm 0.00	0.11 \pm 0.00	0.10 \pm 0.00	0.11 \pm 0.00
	ϵ_{LUMO} \downarrow	0.14 \pm 0.00	0.13 \pm 0.00	0.13 \pm 0.00	0.11 \pm 0.00	0.11 \pm 0.00	0.13 \pm 0.00
	$\Delta\epsilon$ \downarrow	0.18 \pm 0.00	0.17 \pm 0.01	0.19 \pm 0.00	0.16 \pm 0.00	0.16 \pm 0.01	0.19 \pm 0.00
	$\langle R^2 \rangle$ \downarrow	53.03 \pm 4.06	47.81 \pm 3.50	36.14 \pm 0.18	35.17 \pm 0.35	31.65 \pm 1.79	28.57 \pm 0.26
	ZPVE \downarrow	0.24 \pm 0.01	0.14 \pm 0.02	0.08 \pm 0.01	0.06 \pm 0.00	0.06 \pm 0.02	0.03 \pm 0.00
	U_0 \downarrow	609.25 \pm 68.91	329.56 \pm 30.08	143.71 \pm 15.27	100.49 \pm 5.43	31.06 \pm 11.45	9.93 \pm 2.90
	U \downarrow	579.75 \pm 78.19	319.37 \pm 11.63	160.75 \pm 46.21	100.41 \pm 4.27	28.30 \pm 18.81	10.05 \pm 3.18
	H \downarrow	558.89 \pm 71.13	310.95 \pm 20.79	166.10 \pm 41.69	102.85 \pm 4.13	32.18 \pm 11.43	11.05 \pm 6.37
	G \downarrow	580.03 \pm 68.41	320.53 \pm 36.14	166.66 \pm 54.19	102.43 \pm 3.36	19.90 \pm 11.13	10.69 \pm 6.34
	c_v \downarrow	0.90 \pm 0.16	0.64 \pm 0.02	0.53 \pm 0.04	0.39 \pm 0.01	0.47 \pm 0.08	0.17 \pm 0.00
	U_0^{ATOM} \downarrow	3.96 \pm 0.61	1.77 \pm 0.22	1.19 \pm 0.06	0.96 \pm 0.03	0.45 \pm 0.05	0.24 \pm 0.01
	U^{ATOM} \downarrow	4.53 \pm 0.33	1.92 \pm 0.25	1.19 \pm 0.05	0.97 \pm 0.02	0.47 \pm 0.09	0.24 \pm 0.01
	H^{ATOM} \downarrow	3.78 \pm 0.70	1.81 \pm 0.24	1.15 \pm 0.03	0.96 \pm 0.03	0.42 \pm 0.03	0.25 \pm 0.00
	G^{ATOM} \downarrow	3.50 \pm 0.67	1.73 \pm 0.11	1.07 \pm 0.04	0.85 \pm 0.02	0.38 \pm 0.03	0.22 \pm 0.02
	A \downarrow	13.45 \pm 4.20	5.70 \pm 5.79	3.83 \pm 4.08	27.99 \pm 38.02	1.61 \pm 0.19	0.75 \pm 0.11
B \downarrow	0.23 \pm 0.01	0.25 \pm 0.03	0.23 \pm 0.02	0.26 \pm 0.02	0.12 \pm 0.03	0.08 \pm 0.01	
C \downarrow	0.18 \pm 0.03	0.22 \pm 0.03	0.22 \pm 0.07	0.21 \pm 0.02	0.12 \pm 0.02	0.05 \pm 0.01	
MOLNET	FREESOLV \uparrow	0.95 \pm 0.01	0.94 \pm 0.03	0.72 \pm 0.43	0.39 \pm 0.51	0.92 \pm 0.01	0.96 \pm 0.00
	LIPO \uparrow	0.78 \pm 0.01	0.78 \pm 0.01	0.78 \pm 0.01	0.80 \pm 0.01	OOM	0.71 \pm 0.01
	ESOL \uparrow	0.86 \pm 0.01	0.85 \pm 0.01	0.89 \pm 0.01	0.88 \pm 0.01	0.91 \pm 0.01	0.93 \pm 0.01
DOCKSTRING		GAT	GATv2	GIN	PNA	TokenGT	MAGE
	ESR2 \uparrow	0.57 \pm 0.01	0.58 \pm 0.01	0.59 \pm 0.01	0.61 \pm 0.00	0.48 \pm 0.01	0.63 \pm 0.00
	F2 \uparrow	0.79 \pm 0.02	0.83 \pm 0.01	0.85 \pm 0.00	0.85 \pm 0.00	0.77 \pm 0.00	0.88 \pm 0.00
	KIT \uparrow	0.80 \pm 0.00	0.80 \pm 0.00	0.80 \pm 0.01	0.82 \pm 0.00	0.66 \pm 0.02	0.80 \pm 0.00
	PARP1 \uparrow	0.79 \pm 0.04	0.86 \pm 0.01	0.88 \pm 0.00	0.88 \pm 0.00	0.79 \pm 0.01	0.91 \pm 0.00
	PGR \uparrow	0.50 \pm 0.02	0.50 \pm 0.03	0.56 \pm 0.02	0.50 \pm 0.06	0.50 \pm 0.00	0.68 \pm 0.00

Table 4. Test set Matthews correlation coefficient (MCC) for 3 graph-level classification tasks from MoleculeNet, presented as mean \pm standard deviation from 5 different runs. The highest mean values are highlighted in bold. GCN and TokenGT are available in Appendix D.

Dataset	GAT	GATv2	GIN	PNA	Graphormer	MAGE
BBBP \uparrow	0.71 \pm 0.04	0.72 \pm 0.04	0.71 \pm 0.02	0.72 \pm 0.03	OOM	0.76 \pm 0.05
BACE \uparrow	0.59 \pm 0.02	0.60 \pm 0.01	0.56 \pm 0.05	0.45 \pm 0.25	0.09 \pm 0.07	0.65 \pm 0.02
HIV \uparrow	0.38 \pm 0.02	0.38 \pm 0.07	0.35 \pm 0.05	0.38 \pm 0.05	OOM	0.43 \pm 0.02

Despite its simplicity, MAG consistently outperforms other message passing baselines and more involved Transformer-based methods while supporting transfer learning through pre-training and fine-tuning, which does not work well with classical GNNs, and scales favourably in terms of time and memory. Still, several software limitations impede a more efficient MAG implementation (see Appendix A). Compared to Transformers, we remarked several distinguishing features. It performs as well as presented here without any sophisticated learning rate scheduler (warm-up, cosine annealing, etc.) or optimiser. Interestingly, for about half the

datasets MAG performed better with batch normalisation instead of layer normalisation (more in Appendix G). Also, MAG does not use any form of positional encoding, which is against current trends for GNNs and Transformers. Future research might investigate ways to combine node and edge processing, devise efficient attention implementations for graphs, study the importance of positional encodings, integrate successful concepts from other domains such as sparse expert models (Fedus et al., 2022), or study multi-modality.

Table 5. Test set Matthews correlation coefficient (MCC) for graph-level classification tasks from various domains, presented as mean \pm standard deviation from 5 runs. All models use MAGE, except the last 6 (MAGN). The highest mean values are highlighted in bold.

	Dataset	GCN	GAT	GATv2	GIN	PNA	MAG
CV	MALNETTINY \uparrow	0.85 \pm 0.01	0.87 \pm 0.01	0.88 \pm 0.01	0.90 \pm 0.01	0.89 \pm 0.01	0.91 \pm 0.01
	MNIST \uparrow	0.85 \pm 0.00	0.97 \pm 0.00	0.97 \pm 0.00	0.88 \pm 0.01	0.98 \pm 0.00	0.97 \pm 0.00
	CIFAR10 \uparrow	0.46 \pm 0.00	0.63 \pm 0.01	0.63 \pm 0.01	0.44 \pm 0.02	0.65 \pm 0.02	0.63 \pm 0.01
BIOINF.	ENZYMES \uparrow	0.61 \pm 0.03	0.70 \pm 0.04	0.72 \pm 0.03	0.67 \pm 0.04	0.73 \pm 0.02	0.71 \pm 0.03
	PROTEINS \uparrow	0.21 \pm 0.10	0.41 \pm 0.04	0.47 \pm 0.05	0.48 \pm 0.08	0.44 \pm 0.10	0.55 \pm 0.06
	DD \uparrow	0.49 \pm 0.02	0.46 \pm 0.05	0.43 \pm 0.04	0.39 \pm 0.07	0.40 \pm 0.10	0.57 \pm 0.04
SYNTHETIC	SYNTHETIC \uparrow	1.00 \pm 0.00	1.00 \pm 0.00	1.00 \pm 0.00	0.99 \pm 0.03	1.00 \pm 0.00	1.00 \pm 0.00
	SYNTHETIC N. \uparrow	-0.01 \pm 0.05	0.56 \pm 0.12	0.79 \pm 0.11	0.47 \pm 0.14	0.91 \pm 0.03	0.95 \pm 0.03
	SYNTHEIE \uparrow	0.87 \pm 0.04	0.26 \pm 0.07	0.30 \pm 0.07	0.60 \pm 0.07	0.84 \pm 0.08	0.92 \pm 0.05
	TRIANGLES \uparrow	0.17 \pm 0.01	0.15 \pm 0.02	0.14 \pm 0.02	0.15 \pm 0.01	0.07 \pm 0.02	0.22 \pm 0.05
	COLORS-3 \uparrow	0.30 \pm 0.01	0.22 \pm 0.02	0.25 \pm 0.01	0.29 \pm 0.02	0.38 \pm 0.01	0.75 \pm 0.01
SOCIAL	IMDB-BINARY \uparrow	0.59 \pm 0.04	0.52 \pm 0.05	0.51 \pm 0.05	0.54 \pm 0.05	0.50 \pm 0.05	0.62 \pm 0.06
	IMDB-MULTI \uparrow	0.18 \pm 0.03	0.20 \pm 0.02	0.17 \pm 0.01	0.19 \pm 0.02	0.20 \pm 0.02	0.21 \pm 0.03
	REDDIT-BINARY \uparrow	0.54 \pm 0.02	0.53 \pm 0.05	0.35 \pm 0.20	0.49 \pm 0.04	0.53 \pm 0.07	0.61 \pm 0.04
	REDDIT-M-5K \uparrow	0.34 \pm 0.01	0.31 \pm 0.01	0.29 \pm 0.02	0.31 \pm 0.01	0.34 \pm 0.02	0.35 \pm 0.01
	REDDIT-M-12K \uparrow	0.34 \pm 0.01	0.31 \pm 0.01	0.26 \pm 0.02	0.33 \pm 0.00	0.35 \pm 0.01	0.37 \pm 0.03
	TWITCH EGOS \uparrow	0.37 \pm 0.00	0.38 \pm 0.00	0.38 \pm 0.00	0.38 \pm 0.00	0.39 \pm 0.00	0.39 \pm 0.00
	REDDIT THR. \uparrow	0.56 \pm 0.00	0.57 \pm 0.00	0.57 \pm 0.00	0.57 \pm 0.00	0.57 \pm 0.00	0.57 \pm 0.00
	GITHUB STAR. \uparrow	0.27 \pm 0.01	0.30 \pm 0.01	0.21 \pm 0.11	0.28 \pm 0.03	0.36 \pm 0.02	0.31 \pm 0.02

Table 6. Transfer learning performance (RMSE) on QM9 for HOMO and LUMO, presented as mean \pm standard deviation from 5 different runs on test sets. The lowest mean values are highlighted in bold.

Task	Strategy	GCN	GAT	GATv2	GIN	PNA	MAGE
HOMO \downarrow	GW	0.23 \pm 0.004	0.21 \pm 0.002	0.21 \pm 0.002	0.21 \pm 0.001	0.19 \pm 0.001	0.14 \pm 0.001
	Trans.	0.21 \pm 0.001	0.16 \pm 0.000	0.15 \pm 0.000	0.15 \pm 0.000	0.14 \pm 0.000	0.01 \pm 0.000
	Ind.	0.21 \pm 0.001	0.18 \pm 0.000	0.18 \pm 0.000	0.19 \pm 0.000	0.17 \pm 0.000	0.09 \pm 0.000
LUMO \downarrow	GW	0.20 \pm 0.001	0.19 \pm 0.002	0.19 \pm 0.002	0.19 \pm 0.001	0.18 \pm 0.003	0.12 \pm 0.001
	Trans.	0.21 \pm 0.001	0.16 \pm 0.000	0.17 \pm 0.000	0.17 \pm 0.000	0.16 \pm 0.000	0.01 \pm 0.000
	Ind.	0.20 \pm 0.000	0.17 \pm 0.000	0.17 \pm 0.000	0.17 \pm 0.001	0.17 \pm 0.001	0.08 \pm 0.000

Table 7. Average training time per epoch (s) and used memory (GB) for all methods, presented as mean \pm std. from 5 epochs and with the number of parameters (#). For QM9 (103,542 train items), the maximum number of nodes/edges per graph is 29 (MAGN), respectively 56 (MAGE). DD (942 train items) has 5,748 maximum nodes and 28,534 maximum edges. All algorithms use bfloat16 mixed training. (*) Parameters for masked blocks are counted as for normal self-attention, despite a very large number of connections being dropped.

Method	#	QM9		DD	
		Time (s)	Memory (GB)	Time (s)	Memory (GB)
GCN	158K	13.74 \pm 0.47	0.10 \pm 0.00	2.20 \pm 0.11	0.32 \pm 0.02
GAT	10.1M	25.60 \pm 0.35	1.14 \pm 0.07	4.05 \pm 0.08	3.61 \pm 0.55
GATv2	20.1M	28.82 \pm 0.65	1.36 \pm 0.09	5.31 \pm 0.04	5.51 \pm 0.67
GIN	433K	14.95 \pm 1.24	0.12 \pm 0.00	2.13 \pm 0.03	0.28 \pm 0.06
PNA	6.9M	66.62 \pm 1.33	2.53 \pm 0.20	12.05 \pm 0.05	6.77 \pm 0.97
Graphormer	22.3M	186.60 \pm 4.50	1.95 \pm 0.00		OOM
TokenGT	8.1M	30.76 \pm 0.26	1.21 \pm 0.00		OOM
MAGN (naive)	8.3M*	16.46 \pm 0.71	0.31 \pm 0.00		OOM
MAGN (mem-efficient)		15.38 \pm 0.70	0.27 \pm 0.00	13.53 \pm 0.03	1.19 \pm 0.00
MAGE (naive)	8.6M*	26.11 \pm 0.31	0.61 \pm 0.00		OOM
MAGE (mem-efficient)		22.58 \pm 0.49	0.44 \pm 0.00	348.22 \pm 1.32	21.90 \pm 1.19

References

- Alon, U. and Yahav, E. On the bottleneck of graph neural networks and its practical implications. In *International Conference on Learning Representations*, 2021.
- Brody, S., Alon, U., and Yahav, E. How attentive are graph attention networks? In *International Conference on Learning Representations*, 2022.
- Buterez, D., Janet, J. P., Kiddle, S. J., Oglic, D., and Liò, P. Graph neural networks with adaptive readouts. In Oh, A. H., Agarwal, A., Belgrave, D., and Cho, K. (eds.), *Advances in Neural Information Processing Systems*, 2022.
- Buterez, D., Janet, J. P., Kiddle, S. J., and Liò, P. Mf-pcba: Multifidelity high-throughput screening benchmarks for drug discovery and machine learning. *Journal of Chemical Information and Modeling*, 63(9):2667–2678, 2023a. doi: 10.1021/acs.jcim.2c01569. PMID: 37058588.
- Buterez, D., Janet, J. P., Kiddle, S. J., Oglic, D., and Liò, P. Modelling local and general quantum mechanical properties with attention-based pooling. *Communications Chemistry*, 6(1):262, Nov 2023b. ISSN 2399-3669. doi: 10.1038/s42004-023-01045-7.
- Buterez, D., Janet, J. P., Kiddle, S., Oglic, D., and Liò, P. Transfer learning with graph neural networks for improved molecular property prediction in the multifidelity setting. *ChemRxiv*, 2024. doi: 10.26434/chemrxiv-2022-dsbm5-v3.
- Cai, T., Luo, S., Xu, K., He, D., Liu, T.-Y., and Wang, L. Graphnorm: A principled approach to accelerating graph neural network training. In *2021 International Conference on Machine Learning*, May 2021.
- Chen, C., Zuo, Y., Ye, W., Li, X., and Ong, S. P. Learning properties of ordered and disordered materials from multifidelity data. *Nature Computational Science*, 1(1):46–53, 01 2021. ISSN 2662-8457.
- Choromanski, K. M., Likhoshervstov, V., Dohan, D., Song, X., Gane, A., Sarlos, T., Hawkins, P., Davis, J. Q., Mohiuddin, A., Kaiser, L., Belanger, D. B., Colwell, L. J., and Weller, A. Rethinking attention with performers. In *International Conference on Learning Representations*, 2021.
- Corso, G., Cavalleri, L., Beaini, D., Liò, P., and Velickovic, P. Principal neighbourhood aggregation for graph nets. In *Proceedings of the 34th International Conference on Neural Information Processing Systems*, NIPS’20, Red Hook, NY, USA, 2020. Curran Associates Inc. ISBN 9781713829546.
- Dao, T. Flashattention-2: Faster attention with better parallelism and work partitioning, 2023.
- Dao, T., Fu, D. Y., Ermon, S., Rudra, A., and Ré, C. FlashAttention: Fast and memory-efficient exact attention with IO-awareness. In *Advances in Neural Information Processing Systems*, 2022.
- Duvenaud, D., Maclaurin, D., Aguilera-Iparraguirre, J., Gómez-Bombarelli, R., Hirzel, T., Aspuru-Guzik, A., and Adams, R. P. Convolutional networks on graphs for learning molecular fingerprints. In *Proceedings of the 28th International Conference on Neural Information Processing Systems - Volume 2*, NIPS’15, pp. 2224–2232, Cambridge, MA, USA, 2015. MIT Press.
- Dwivedi, V. P., Rampásek, L., Galkin, M., Parviz, A., Wolf, G., Luu, A. T., and Beaini, D. Long range graph benchmark. In *Thirty-sixth Conference on Neural Information Processing Systems Datasets and Benchmarks Track*, 2022.
- Fedai, A., Reiser, P., Peña, J. E. O., Friederich, P., and Wenzel, W. Accurate gw frontier orbital energies of 134 kilo molecules. *Scientific Data*, 10(1):581, Sep 2023. ISSN 2052-4463. doi: 10.1038/s41597-023-02486-4.
- Fedus, W., Dean, J., and Zoph, B. A review of sparse expert models in deep learning, 2022.
- García-Ortegón, M., Simm, G. N. C., Tripp, A. J., Hernández-Lobato, J. M., Bender, A., and Bacallado, S. Dockstring: Easy molecular docking yields better benchmarks for ligand design. *Journal of Chemical Information and Modeling*, 62(15):3486–3502, 2022. doi: 10.1021/acs.jcim.1c01334. PMID: 35849793.
- Gilmer, J., Schoenholz, S. S., Riley, P. F., Vinyals, O., and Dahl, G. E. Neural message passing for quantum chemistry. In *Proceedings of the 34th International Conference on Machine Learning - Volume 70*, ICML’17, pp. 1263–1272. JMLR.org, 2017.
- Godwin, J., Schaarschmidt, M., Gaunt, A. L., Sanchez-Gonzalez, A., Rubanova, Y., Veličković, P., Kirkpatrick, J., and Battaglia, P. Simple GNN regularisation for 3d molecular property prediction and beyond. In *International Conference on Learning Representations*, 2022.
- Hu, W., Liu, B., Gomes, J., Zitnik, M., Liang, P., Pande, V., and Leskovec, J. Strategies for pre-training graph neural networks. In *International Conference on Learning Representations*, 2020.
- Jain, P., Wu, Z., Wright, M. A., Mirhoseini, A., Gonzalez, J. E., and Stoica, I. Representing long-range context for graph neural networks with global attention. In Beygelzimer, A., Dauphin, Y., Liang, P., and Vaughan, J. W. (eds.), *Advances in Neural Information Processing Systems*, 2021.

- Kearnes, S., McCloskey, K., Berndl, M., Pande, V., and Riley, P. Molecular graph convolutions: moving beyond fingerprints. *Journal of Computer-Aided Molecular Design*, 30(8):595–608, Aug 2016. ISSN 1573-4951. doi: 10.1007/s10822-016-9938-8.
- Kim, J., Nguyen, D. T., Min, S., Cho, S., Lee, M., Lee, H., and Hong, S. Pure transformers are powerful graph learners. In Oh, A. H., Agarwal, A., Belgrave, D., and Cho, K. (eds.), *Advances in Neural Information Processing Systems*, 2022.
- Kreuzer, D., Beaini, D., Hamilton, W. L., Létourneau, V., and Tossou, P. Rethinking graph transformers with spectral attention. In Beygelzimer, A., Dauphin, Y., Liang, P., and Vaughan, J. W. (eds.), *Advances in Neural Information Processing Systems*, 2021.
- Lee, J., Lee, Y., Kim, J., Kosiorok, A., Choi, S., and Teh, Y. W. Set transformer: A framework for attention-based permutation-invariant neural networks. In *Proceedings of the 36th International Conference on Machine Learning*, pp. 3744–3753, 2019.
- Lefaudeux, B., Massa, F., Liskovich, D., Xiong, W., Caggiano, V., Naren, S., Xu, M., Hu, J., Tintore, M., Zhang, S., Labatut, P., and Haziza, D. xformers: A modular and hackable transformer modelling library. <https://github.com/facebookresearch/xformers>, 2022.
- Loshchilov, I. and Hutter, F. Decoupled weight decay regularization. In *International Conference on Learning Representations*, 2019.
- Paszke, A., Gross, S., Massa, F., Lerer, A., Bradbury, J., Chanan, G., Killeen, T., Lin, Z., Gimelshein, N., Antiga, L., Desmaison, A., Kopf, A., Yang, E., DeVito, Z., Raison, M., Tejani, A., Chilamkurthy, S., Steiner, B., Fang, L., Bai, J., and Chintala, S. Pytorch: An imperative style, high-performance deep learning library. In *Advances in Neural Information Processing Systems 32*, pp. 8024–8035. Curran Associates, Inc., 2019.
- Rabe, M. N. and Staats, C. Self-attention does not need $o(n^2)$ memory. *CoRR*, abs/2112.05682, 2021.
- Ramakrishnan, R., Dral, P. O., Rupp, M., and von Lilienfeld, O. A. Quantum chemistry structures and properties of 134 kilo molecules. *Scientific Data*, 1(1):140022, Aug 2014. ISSN 2052-4463. doi: 10.1038/sdata.2014.22.
- Rampásek, L., Galkin, M., Dwivedi, V. P., Luu, A. T., Wolf, G., and Beaini, D. Recipe for a general, powerful, scalable graph transformer. In Oh, A. H., Agarwal, A., Belgrave, D., and Cho, K. (eds.), *Advances in Neural Information Processing Systems*, 2022.
- Rampásek, L., Galkin, M., Dwivedi, V. P., Luu, A. T., Wolf, G., and Beaini, D. Recipe for a General, Powerful, Scalable Graph Transformer. *Advances in Neural Information Processing Systems*, 35, 2022.
- Shazeer, N. GLU variants improve transformer. *CoRR*, abs/2002.05202, 2020.
- Shirzad, H., Velingker, A., Venkatachalam, B., Sutherland, D. J., and Sinop, A. K. Exphormer: Scaling graph transformers with expander graphs, 2023.
- Tönshoff, J., Ritzert, M., Rosenbluth, E., and Grohe, M. Where did the gap go? reassessing the long-range graph benchmark. In *The Second Learning on Graphs Conference*, 2023.
- Vaswani, A., Shazeer, N., Parmar, N., Uszkoreit, J., Jones, L., Gomez, A. N., Kaiser, L. u., and Polosukhin, I. Attention is all you need. In Guyon, I., Luxburg, U. V., Bengio, S., Wallach, H., Fergus, R., Vishwanathan, S., and Garnett, R. (eds.), *Advances in Neural Information Processing Systems*, volume 30. Curran Associates, Inc., 2017.
- Veličković, P., Cucurull, G., Casanova, A., Romero, A., Liò, P., and Bengio, Y. Graph attention networks. In *International Conference on Learning Representations*, 2018.
- Wolf, T., Debut, L., Sanh, V., Chaumond, J., Delangue, C., Moi, A., Cistac, P., Rault, T., Louf, R., Funtowicz, M., Davison, J., Shleifer, S., von Platen, P., Ma, C., Jernite, Y., Plu, J., Xu, C., Le Scao, T., Gugger, S., Drame, M., Lhoest, Q., and Rush, A. Transformers: State-of-the-art natural language processing. In Liu, Q. and Schlangen, D. (eds.), *Proceedings of the 2020 Conference on Empirical Methods in Natural Language Processing: System Demonstrations*, pp. 38–45, Online, October 2020. Association for Computational Linguistics. doi: 10.18653/v1/2020.emnlp-demos.6.
- Xiong, R., Yang, Y., He, D., Zheng, K., Zheng, S., Xing, C., Zhang, H., Lan, Y., Wang, L., and Liu, T.-Y. On layer normalization in the transformer architecture. In *Proceedings of the 37th International Conference on Machine Learning*, ICML’20. JMLR.org, 2020a.
- Xiong, Z., Wang, D., Liu, X., Zhong, F., Wan, X., Li, X., Li, Z., Luo, X., Chen, K., Jiang, H., and Zheng, M. Pushing the boundaries of molecular representation for drug discovery with the graph attention mechanism. *Journal of Medicinal Chemistry*, 63(16):8749–8760, 2020b. doi: 10.1021/acs.jmedchem.9b00959. PMID: 31408336.
- Ying, C., Cai, T., Luo, S., Zheng, S., Ke, G., He, D., Shen, Y., and Liu, T.-Y. Do transformers really perform badly

for graph representation? In *Thirty-Fifth Conference on Neural Information Processing Systems*, 2021.

Zaheer, M., Guruganesh, G., Dubey, K. A., Ainslie, J., Alberti, C., Ontanon, S., Pham, P., Ravula, A., Wang, Q., Yang, L., and Ahmed, A. Big bird: Transformers for longer sequences. In Larochelle, H., Ranzato, M., Hadsell, R., Balcan, M., and Lin, H. (eds.), *Advances in Neural Information Processing Systems*, volume 33, pp. 17283–17297. Curran Associates, Inc., 2020.

Zhao, L. and Akoglu, L. Pairnorm: Tackling oversmoothing in gnns. In *International Conference on Learning Representations*, 2020.

A. Limitations

In terms of limitations, we highlight that the available libraries are not optimised for masking or custom attention patterns. This is most evident for very dense graphs (tens of thousands of edges or more). Memory efficient and Flash attention are available natively in PyTorch (Paszke et al., 2019) starting from version 2, as well as in the xFormers library (Lefaudeux et al., 2022). More specifically, we have tested at least 5 different implementations of MAG: (1) leveraging the `MultiheadAttention` module from PyTorch, (2) leveraging the `MultiHeadDispatch` module from xFormers, (3) a manual implementation of multihead attention, relying on PyTorch’s `scaled_dot_product_attention` function, (4) a manual implementation of multihead attention, relying on xFormers’ `memory_efficient_attention`, and (5) a naive implementation. Options (1) - (4) can all make use of efficient and fast implementations. However, we have observed performance differences between the 4 implementations, as well as compared to a naive implementation. This behaviour is likely due to the different low-level kernel implementations. Moreover, Flash attention does not support custom attention masks as there is little interest for such functionality from a language modelling perspective.

Although the masks can be computed efficiently during training, all frameworks require the last two dimensions of the input mask tensor to be of shape (N_d, N_d) for nodes or (N_e, N_e) for edges, effectively squaring the number of nodes or edges. However, the mask tensors are very sparse and a sparse tensor alternative could greatly reduce the memory consumption for large and dense graphs. Such an option exists for the PyTorch native attention, but it is currently broken.

Another possible optimisation would be to use nested (ragged) tensors to represent graphs, since padding is currently necessary to ensure identical dimensions for attention. A prototype nested tensor attention is available in PyTorch; however, not all the required operations are supported and converting between normal and nested tensors is slow.

For all implementations, it is required that the mask tensor is repeated by the number of attention heads (e.g. 8 or 16). However, a notable bottleneck is encountered for the `MultiheadAttention` and `MultiHeadDispatch` variants described above, which require that the repeats happen in the batch dimension, i.e. requiring 3D mask tensors of shape $(B \times H, N, N)$, where H is the number of heads. The other two efficient implementations require a 4D mask instead, i.e. (B, H, N, N) , where one can use PyTorch’s `expand` function instead of `repeat`. The `expand` alternative does not use any additional memory, while `repeat` requires $\times H$ memory. Note that it is not possible to reshape the 4D tensor created using `expand` without using additional memory.

B. Helper functions

`consecutive` is a helper function that generates consecutive numbers starting from 0, with a length specified in its tensor argument as the difference between adjacent elements, and a second integer argument used for the last length computation, e.g. `consecutive([1, 4, 6], 10) = [0, 1, 2, 0, 1, 0, 1, 2, 3]`, and `first_unique_index` finds the first occurrence of each unique element in the tensor (sorted), e.g. `first_unique_index([3, 2, 3, 4, 2]) = [1, 0, 3]`.

C. Experimental setup

We follow a simple and universal experimental protocol to ensure that it is possible to compare the results of different methods and to evaluate a large number of datasets with high throughput. We chose a number of reasonable hyperparameters and settings for all methods, regardless of their nature (GNN or attention-based). This includes the AdamW optimiser (Loshchilov & Hutter, 2019), learning rate (0.0001), batch size (128), 32-bit training (without mixed precision), early stopping with a patience of 30 epochs (100 for the very small datasets such as FREESOLV), and gradient clipping (set to the default value of 0.5). Furthermore, we used a simple learning rate scheduler that halved the learning rate if no improvement was encountered for 15 epochs (half the early stopping patience).

For GNNs, we used 4 graph layers for all algorithms (GCN, GIN, GAT, GATv2, PNA) and the mean readout function, a node dimension of 64, and a hidden dimension for the graph layers of 256. All layers use batch normalisation. Settings specific to some algorithms were also given by reasonable defaults, such as 8 attention heads for GAT(v2), and 5 towers for PNA. In certain instances such as small datasets with dense graphs, the defaults selected above can lead to out-of-memory errors, even for GNNs, in particular the more computationally-intensive algorithms such as GAT(v2) or PNA. In such cases, we lower the settings that were the most likely cause, such as the hidden dimension or batch size, to the next (lower) power of two. In some cases, mixed precision training (using the `bfloat16` type) was performed as an alternative if Ampere-class GPUs were available.

For Graphormer and TokenGT, we leverage the `huggingface` (Wolf et al., 2020) implementation. Our selection of reasonable defaults include 3 layers, a hidden and embedding size of 512, and 8 attention heads, in addition to the defaults mentioned earlier such as learning rate and batch size. Graphormer in particular can be difficult to train, and in such cases we reduce the complexity of the model using the same strategies as above. However, note that many out-of-memory errors for this family of models are not due to GPU memory, but RAM; we attempted to use up to 256GB, but conceded if it did not work.

For MAG, the same suite of “general” defaults such as the learning rate and batch size apply. We also generally follow the same configuration for all datasets. However, since MAG is a new architecture with many unknowns, we generally evaluate a small number of variations for each dataset and select the best one according to the validation metrics. The variations typically involve choosing MAGN or MAGE, batch or layer normalisation, the number (3 or 4) and order of self-attention and masked self attention blocks (e.g. SMM, MSMM, etc.), the hidden size (256 or 512) and the number of attention heads (8 or 16). We generally prefer MAGE in all situations and only consider MAGN for datasets where MAGE would take a very long time to run or requires heavy modifications to the default parameters. This is because MAGE can naturally incorporate edge features and almost always performs better. We have also found SwiGLU to often be better than plain MLPs (Shazeer, 2020).

Graphormer (and TokenGT to a lower extent) have very expensive pre-processing steps which require up to hundreds of GBs of storage space to cache intermediary results. The alternative would be to not use caching; however, this means that everything must be stored in memory, resulting in almost immediate crashing. As a further complication, for large datasets such as DOCKSTRING, Graphormer would run for a few epochs but spontaneously crash, most likely due to high memory utilisation during training. Combined with the fact that one epoch took several hours, we have included Graphormer results only for a minority of datasets.

Hyperparameter optimisation

Other than the basic filtering described above for MAG, we did not use any techniques for tuning. In particular, we did not perform hyperparameter optimisation and have not tuned aspects of the networks such as the optimiser, learning rate, batch size, dropout, hidden dimensions, etc. We acknowledge that we are not using optimal parameters for the majority of models. However, this is also true for MAG, and tuning every model presented here would dramatically increase the time and resource utilisation (as well as the financial costs associated with it), defeating the purpose of presenting a simple yet effective alternative to GNNs.

Evaluation

Generally, for a self-contained evaluation we split all datasets using a random 80%, 10%, 10% split for train, validation, and test. The same data splits are used for the different evaluated algorithms. Some datasets, such as MNIST or DOCKSTRING are provided with existing train, test, and optionally validation splits. If such splits are available through PyTorch Geometric or from the authors (such as DOCKSTRING), we use them and we do not perform our own random splits. For all datasets and models, we provide

results from 5 different runs (seeds).

D. Additional results

The missing GCN, TokenGT, and Graphormer results for some of the datasets presented in the main text are presented below in Tables 8 and 9. These complete the results from Tables 3 and 4.

Table 8. Test set root mean squared error (RMSE) for QM9 and R^2 for the others, for GCN and TokenGT, presented as mean \pm standard deviation from 5 different runs.

	Property	GCN	TokenGT
QM9	μ	0.67 \pm 0.01	1.00 \pm 0.00
	α	3.51 \pm 0.18	2.14 \pm 0.07
	ϵ_{HOMO}	0.14 \pm 0.00	0.26 \pm 0.01
	ϵ_{LUMO}	0.15 \pm 0.00	0.42 \pm 0.01
	$\Delta\epsilon$	0.21 \pm 0.00	0.56 \pm 0.01
	$\langle R^2 \rangle$	67.74 \pm 5.72	177.70 \pm 6.39
	ZPVE	0.23 \pm 0.00	0.14 \pm 0.00
	U_0	573.32 \pm 47.41	228.49 \pm 198.10
	U	594.55 \pm 57.81	228.49 \pm 198.10
	H	575.10 \pm 48.66	228.49 \pm 198.10
	G	594.07 \pm 57.00	228.49 \pm 198.10
	c_v	1.34 \pm 0.26	1.05 \pm 0.03
	U_0^{ATOM}	3.99 \pm 0.04	2.02 \pm 0.30
	U^{ATOM}	4.19 \pm 0.33	2.22 \pm 0.19
	H^{ATOM}	4.05 \pm 0.02	2.16 \pm 0.10
	G^{ATOM}	3.70 \pm 0.02	1.91 \pm 0.14
	A	1.17 \pm 0.11	0.01 \pm 0.01
B	0.28 \pm 0.02	0.40 \pm 5.80	
C	0.24 \pm 0.02	0.35 \pm 2.36	
MOLNET	Freesolv	0.34 \pm 0.51	0.86 \pm 0.02
	LIPO	0.71 \pm 0.01	OOM
	ESOL	0.86 \pm 0.01	0.78 \pm 0.01
DOCKSTRING		GCN	Graphormer
	ESR2	0.53 \pm 0.01	OOM
	F2	0.78 \pm 0.00	OOM
	KIT	0.76 \pm 0.00	OOM
	PARP1	0.81 \pm 0.00	OOM
PGR	0.36 \pm 0.01	OOM	

Table 9. Test set Matthews correlation coefficient (MCC) for GCN and TokenGT for 3 graph-level classification tasks from MoleculeNet, presented as mean \pm standard deviation, over 5 runs.

Dataset	GCN	TokenGT
BACE	0.35 \pm 0.31	0.19 \pm 0.09
BBBP	0.68 \pm 0.02	0.31 \pm 0.09
HIV	0.39 \pm 0.03	OOM

E. Dataset statistics

We present a summary of all the used datasets, along with their size and the maximum number of nodes and edges encountered in a graph in the dataset (Table 10). The last two are important as they determine the shape of the mask and of the inputs for the attention blocks. Technically, we require that the maximum number of nodes/edges is determined per batch and the tensors to be padded accordingly. This per-batch maximum is lower than the dataset maximum for most batches. However, certain operations such as layer norm., if performed over the last two dimensions, require a constant value. To enable this, we use the dataset maximum.

Table 10. Summary of used datasets, their size, and the max. number of nodes (**N**) and edges (**E**) seen in a graph in the dataset.

	Dataset	Size	N	E
LRGB	PEPT-STRUCT	15 535	444	928
	PEPT-FUNC	15 535	444	928
NODE	PPI	24	3 480	106 754
	CORA	1	2 708	10 556
	CITeseER	1	3 327	9 104
	QM9	133 885	29	56
MOLECULENET	Freesolv	642	44	92
	LIPO	4 200	216	438
	ESOL	1 128	119	252
	BBBP	2 039	269	562
	BACE	1 513	184	376
	HIV	41 127	438	882
	DOCKSTRING	260 060	164	342
	MALNETTINY	5 000	4 994	20 096
CV	MNIST	70 000	75	600
	CIFAR10	60 000	150	1 200
BIOINFO	ENZYMES	600	126	298
	PROTEINS	1 113	620	2 098
	DD	1 178	5 748	28 534
SYNTHETIC	SYNTHETIC	300	100	392
	SYNTHETIC NEW	300	100	396
	SYNTHIE	400	100	424
	TRIANGLES	45 000	100	396
	COLORS-3	10 500	200	794
SOCIAL	IMDB-BINARY	1 000	136	2 498
	IMDB-MULTI	1 500	89	2 934
	REDDIT-BINARY	2 000	3 782	8 142
	REDDIT-M-5K	4 999	3 648	9 566
	REDDIT-M-12K	11 929	3 782	10 342
	TWITCH EGOS	127 094	52	1 572
	REDDIT THR.	203 088	97	370
	GITHUB STAR.	12 725	957	9 336

F. Masked attention equation

Masked attention can be thought of as a custom attention pattern, which for graphs was described succinctly by (Shirzad et al., 2023). An adaptation for masking would be:

$$\text{MaskedSelfAttention}(\mathbf{X}, \mathbf{M}) = \sum_{j=1}^h \mathbf{W}_O^j \left(\mathbf{W}_V^j \mathbf{X}_M \right) \sigma \left(\left(\mathbf{W}_K^j \mathbf{X}_M \right)^T \left(\mathbf{W}_Q^j \mathbf{X}_M \right) \right) \quad (7)$$

where h is the number of attention heads, \mathbf{X} is the input features matrix, \mathbf{M} is the custom attention pattern/mask, which restricts the attention to a subset of elements of \mathbf{X} , denoted by \mathbf{X}_M , \mathbf{W}_Q^j , \mathbf{W}_K^j , \mathbf{W}_V^j , \mathbf{W}_O^j are weight matrices corresponding to queries, keys, values, and outputs, respectively, and σ is the softmax function.

G. Layer vs batch normalisation

Contrary to standard Transformers and current trends, we have found that simply replacing the layer normalisation (LN) operation within MAG with batch normalisation (BN) can dramatically improve performance on a number of datasets. LN was our default initial choice and we have found that it works better for the standard QM9 dataset and its properties (Table 3). For the other datasets and tasks (excluding the 19 QM9 properties but including the QM9 GW tasks from Table 6 and the PEPT-STRUCT and PEPT-FN datasets), although we have not exhaustively tested LN vs BN models, we have generally observed that LN is preferable for 20 tasks and BN for 17. More specifically, BN was preferable for the DOCKSTRING properties PARP1, ESR2, and PGR, as well as for the datasets: CIFAR10, COLORS-3, DD, ESOL, LIPO, PEPT-STRUCT, PEPT-FN, PROTEINS, REDDIT THREADS, REDDIT-MULTI-12K, SYNTHIE, TRIANGLES, ENZYMES, and TWITCH EGOS. Apart from the fact that most molecular datasets tend to do better with LN, there is no obvious indication of which normalisation technique might be preferable for certain dataset types.

H. Experimental platform

Representative versions of the software used as part of this paper include Python 3.11.6, PyTorch version 2.1.1 with CUDA 11.8, PyTorch Geometric 2.4.0, PyTorch Lightning 1.9.5, huggingface transformers version 4.35.2, and xFormers version 0.0.23. We have also tested our code with CUDA ≥ 12.0 . It is worth noting that attention masking and efficient implementations of attention are early features that are advancing quickly. This means that their behaviour might change unexpectedly and there might be bugs. For example, PyTorch 2.1.1 recently [fixed a bug](#) that concerned non-contiguous custom attention masks in the `scaled_dot_product_attention` function.

In terms of hardware, the GPUs used include an NVIDIA RTX 3090 with 24GB VRAM, NVIDIA V100 with 16GB or 32GB of VRAM, and NVIDIA A100 with 40GB of VRAM. Recent, efficient implementations of attention are optimised for the newest GPU architectures, generally starting from Ampere (RTX 3090 and A100). However, while slower, it is possible to run memory efficient attention on V100 GPUs.

I. Multiple configurations of MAGE

We summarise the results of running MAGE on the QM9 property α (alpha) in Table 11. Compared to the main results of Table 3, we used an early stopping patience of 10 epochs and trained for a maximum of 150 epochs.

The configurations are given as a sequence of masked attention (M) or self-attention (S) blocks, followed by a pooling by multihead attention block (P). While performance is slightly lower than Table 3 due to the training changes, we notice that models that use exclusively self-attention blocks and no masked blocks are worse than models that predominantly rely on masked attention, as expected. It is also possible to use self-attention blocks after pooling by multihead attention. However, that would greatly increase the number of possible configurations and we do not evaluate this option here.

Table 11. Test set RMSE for MAGE configurations for α (QM9), presented as mean \pm standard deviation from 5 different runs.

Configuration	MAGE
MMMSP	0.499 \pm 0.012
MMSSP	0.501 \pm 0.007
MMSP	0.503 \pm 0.010
MMSMP	0.506 \pm 0.003
MSMMP	0.508 \pm 0.010
MMMMP	0.509 \pm 0.007
MSSMP	0.509 \pm 0.004
SMSSP	0.513 \pm 0.012
SMMSP	0.515 \pm 0.008
MSSSP	0.517 \pm 0.014
MSMP	0.518 \pm 0.008
MSMSP	0.519 \pm 0.010
SMSMP	0.520 \pm 0.010
SMMMP	0.522 \pm 0.010
MMMP	0.522 \pm 0.003
SSMMP	0.525 \pm 0.012
MSP	0.525 \pm 0.008
MSSP	0.527 \pm 0.015
SMMP	0.527 \pm 0.017
SSMSP	0.528 \pm 0.009
SMSP	0.530 \pm 0.005
SSSMP	0.539 \pm 0.014
MMP	0.545 \pm 0.017
SSMP	0.546 \pm 0.010
MP	0.561 \pm 0.007
SMP	0.567 \pm 0.011
SSSSP	0.590 \pm 0.014
SSSP	0.604 \pm 0.013
SSP	0.642 \pm 0.013
SP	0.665 \pm 0.026